Available online at www.sciencedirect.com

SciVerse ScienceDirect

Ceramics International 39 (2013) 7523–7529

CERAMICS INTERNATIONAL

www.elsevier.com/locate/ceramint

Synthesis, structural and luminescence properties of near white light emitting Dy^{3+}-doped Y_2CaZnO_5 nanophosphor for solid state lighting

R. Rajeswari[a], C.K. Jayasankar[a,*], D. Ramachari[a], S. Surendra Babu[b]

[a]Department of Physics, Sri Venkateswara University, Tirupati 517502, India
[b]Directorate of Laser Systems, Research Centre Imarat, Hyderabad 500069, India

Received 2 February 2013; received in revised form 3 March 2013; accepted 4 March 2013
Available online 15 March 2013

Abstract

Novel near white light emitting Y_2CaZnO_5 (YCZ) nanocrystalline powders doped with Dy^{3+} ions were synthesized via the citrate gel combustion method. The structure of the compound is found to be triclinic with a particle size in the range of 20–30 nm. Luminescence properties have been characterized using photoluminescence (PL), excitation spectra and decay time measurements. The PL spectra have shown a broad blue band due to $^4F_{9/2}\rightarrow{}^6H_{15/2}$ transition and sharp yellow band corresponding to $^4F_{9/2}\rightarrow{}^6H_{13/2}$ transition of Dy^{3+} ions. From the concentration dependent PL studies, the optimum concentration of Dy^{3+} ions in YCZ is found to be 1.0 mol%, where intense near white light emission was observed. The Dy^{3+}:YCZ nanophosphor has shown relatively better white color properties than the reported Dy^{3+}:Y_2O_3 nanophosphor. The yellow to blue intensity ratios, CIE chromaticity coordinates and correlated color temperature studies have shown the possibility of using this compound for white light emission.

Keywords: A. Sol–gel process; B. Spectroscopy; C. Lifetime; C. Optical properties

1. Introduction

Solid-state lighting (SSL) has the potential to revolutionize the lighting market through the introduction of highly energy-efficient, longer-lasting, versatile light sources, including high-quality white light. The combined efforts of government and industries all over the world have accelerated the advances of white-light SSL devices for general lighting at a rapid pace. Generally, white light emitting diode (w-LED) architecture consists of a blue or near-ultraviolet (n-UV) semiconductor light emitting element having a photoluminescence phosphor coated on it [1]. By far, the major work during the past focused on the Ce^{3+} and Eu^{2+}/Eu^{3+}-activated luminescent compounds, because they have proven to be the efficient commercial phosphors used in display devices, and w-LEDs in solid state lighting [2–4]. Being an efficient white light emitting combination, they suffer from drawbacks such as individual degradation of lifetime for phosphor and LEDs and poor white light performance. To overcome these problems, the exploration of novel phosphor materials plays an important role in the development of w-LEDs. Besides cerium and europium ions, dysprosium (Dy^{3+}) is another interesting activator, both in the visible and NIR regions. The Dy^{3+} ions emit intense blue and yellow colors under n-UV or blue excitation, which can be further fine tuned through the variation of the Dy^{3+} concentration to yield white color. The yellow to blue intensity ratio and CIE chromaticity coordinates obtained for the recent Dy^{3+}-doped inorganic compounds have revealed the potentiality of these compounds for the development of phosphor for w-LEDs [5–10].

Conventionally, phosphor powders were prepared by the solid-state reaction at high temperature. Although simple to operate, this method has several disadvantages including high-temperature processing, long calcination time and repeated milling and grinding which may lead to the contamination of the final product. To overcome these disadvantages, several solution-based synthesis techniques, such as sol–gel, co-precipitation, spray pyrolysis and the hydrothermal methods have been developed [11]. In the present work, synthesis, structural and luminescent properties of novel Dy^{3+}-doped Y_2CaZnO_5 (YCZ) nanophosphor were investigated. The synthesis method

*Corresponding author. Tel.: +91 877 2248033; fax: +91 877 2289472.
E-mail address: ckjaya@yahoo.com (C.K. Jayasankar).

0272-8842/$ - see front matter © 2013 Elsevier Ltd and Techna Group S.r.l. All rights reserved.
http://dx.doi.org/10.1016/j.ceramint.2013.03.003

proposed in the present work is simple, affordable, and versatile compared to the other existing chemical routes and can be followed even for the mass production of nanophosphors of this class. The spectroscopic and white light properties for various concentrations of Dy^{3+} ions were investigated in detail and the results were compared with the reported systems.

2. Experimental details

Y_2CaZnO_5 (YCZ) nanophosphor doped with various Dy^{3+} ion concentrations (0.1, 0.5, 1.0, 2.5, 5.0 and 7.5 mol%) were prepared by the modified citrate gel combustion method. High-purity Y_2O_3, ZnO, $CaCO_3$, Dy_2O_3 and $C_6H_8O_7$ (citric acid) from Sigma-Aldrich were taken as starting materials. In a typical experiment, stoichiometric amounts of all the oxides and carbonates were dissolved in concentrated nitric acid to make $Y(NO_3)_3$, $Zn(NO_3)_2$, $Ca(NO_3)_2$ and $Dy(NO_3)_3$. These nitrate precursors were added with citric acid, which was dissolved in water (by adjusting the ratio of citric acid to metal nitrates as 4:1). Citric acid acts as the monomer to form a transparent complex gel upon drying for 12 h in an oven at 75 °C. Then the gel was taken in a quartz boat and introduced in a pre-heated furnace at 800 °C. Initially the citrate complex gel transforms to a black fluffy mass nearly ten times the gel volume and starts decomposing to CO_2 and H_2O vapors. After 15–30 min a white voluminous mass of the YCZ:Dy^{3+} nanophosphor is obtained which could easily be crushed to ultra-fine powder used for further characterization. Synthesis of size-controlled nanophosphor particles with high yield (~90%) is one of the highlights of this method.

Crystalline structure of the prepared samples were characterized by using a Bruker D-8 advanced powder X-ray diffractometer with Cu Kα radiation operated at 35 kV and 30 mA. Compositional analysis has been carried out using a Hitachi VP-SEM S-3400 N Scanning Electron Microscope. TEM images were collected using a Tecnai G2 F30 S-Twin (FEI; Super Twin lens with $Cs = 1.2$ mm) instrument operating at an accelerating voltage of 300 kV, having a point resolution of 0.2 nm and lattice resolution of 0.14 nm. Fourier-transform infrared (FTIR) transmission spectra, with a spectral resolution of 2 cm^{-1}, were measured using a Perkin-Elmer Paragon 500 FTIR spectrometer. The room temperature photoluminescence (PL), excitation spectra with a resolution of 0.5 nm and decay time measurements with a temporal resolution of 0.01 ms were carried out using a Jobin Yvon Fluorlog-3 spectrofluorimeter equipped with a xenon arc lamp.

3. Results and discussion

3.1. Structural analysis

For comparison of the crystal structure, the bulk YCZ material was prepared by the conventional solid state reaction method, at a sintering temperature of 1300 °C for 12 h. Fig. 1 shows the XRD pattern of bulk YCZ and 1.0 mol% Dy_2O_3 doped YCZ nanophosphors prepared by the sol–gel combustion method. Since the material, Y_2CaZnO_5 (YCZ), under study is an entirely new lattice and the respective JCPDS data is not available, WIN-INDEX (ver. 3.08) software has been used for the structural refinement studies and determined (*h k l*) values corresponding to the crystalline planes. The XRD patterns of both bulk YCZ and nanocrystalline YCZ:Dy^{3+} samples are identical with respect to the line positions and relative intensities. The diffraction lines of the nanocrystalline material are broadened due to the small particle size. The structure of both the bulk YCZ and nanocrystalline YCZ:Dy^{3+} phosphors is found to be triclinic. The unit cell parameters of nanocrystalline YCZ:Dy^{3+} (bulk YCZ) are found to be $a = 10.02$ Å (7.45 Å); $b = 12.68$ Å (12.58 Å); $c = 11.27$ Å (5.53 Å); $\alpha = 132.14°$ (97.31°); $\beta = 117.93°$ (94.57°); $\gamma = 50.20°$ (100.27°) and volume of 813.95 $Å^3$ (503.57 $Å^3$). The crystallite size of the material was calculated using the Scherrer formula

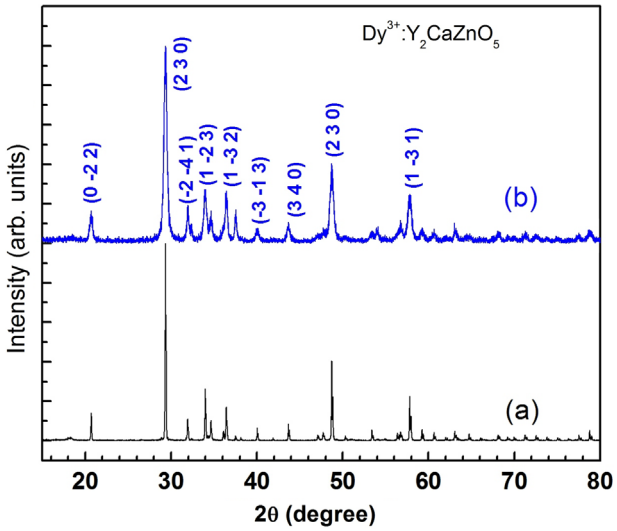

Fig. 1. XRD patterns of (a) bulk and (b) 1.0 mol% Dy_2O_3-doped Y_2CaZnO_5 nanophosphors. The (*h k l*) values generated from WIN-INDEX (ver. 3.08) software are shown in the figure.

$$D = \frac{K\lambda}{\beta cos\theta} \quad (1)$$

where D is the crystallite size, K is the dimensionless shape factor (0.9), λ is the X-ray wavelength, β is the FWHM and θ is the Bragg angle. The crystallite diameter of the samples prepared by the combustion method is found to be 21 nm.

The FTIR spectral studies were carried out to study the functional groups in the YCZ host. Fig. 2 shows the FTIR spectra of bulk YCZ, 0.5 mol% and 7.5 mol% Dy_2O_3 doped YCZ nanophosphor samples. As can be seen from the figure major transmission bands were observed at 3413, 2918, 1441, 1078 and 872 cm^{-1}. The broad IR transmission band found for all the studied samples at 3413 cm^{-1} is due to the stretching vibration of the hydroxyl group (OH^-) of absorbed water molecules. The sharp peaks at 2918 cm^{-1} are associated with the symmetric and anti-symmetric stretch vibrations of the C–H and CO groups. The transmission peaks located from 1440 to 1700 cm^{-1} can be assigned to the stretching vibrations of COO^-. The bands observed at 872 cm^{-1} are assigned to be the Y–O

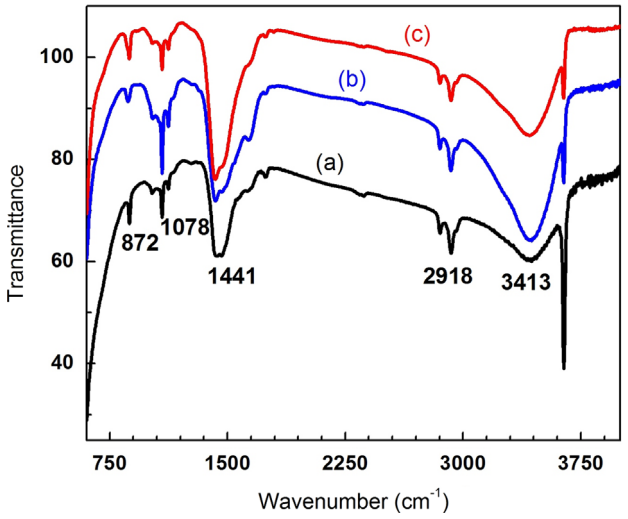

Fig. 2. FTIR spectra of (a) bulk, (b) 0.5 mol% and (c) 7.5 mol% Dy_2O_3-doped Y_2CaZnO_5 nanophosphors.

stretching vibrations, which also confirms the formation of the YCZ nanopowder via the sol–gel combustion technique [12].

Fig. 3(a) shows the energy dispersive X-ray analysis (EDAX) and the inset shows the Scanning Electron Microscopy (SEM) image of the 1.0 mol% Dy_2O_3 doped YCZ nanophosphors sample. The nanophosphor consists of all the elements such as Y, Dy, Zn, Ca and O present in respective proportions with a uniform distribution of the particles. Typical TEM image for 1.0 mol% Dy_2O_3 doped YCZ nanophosphors is shown in Fig. 3(b). Fluffy, voluminous and delicate porous nanophosphor samples are formed due to the evolution of a large amount of gases during the self-proliferating sol–gel combustion reaction. As can be seen from the image, the grain size of the samples prepared by the modified citrate gel method is in the nanoscale range. Loosely bound agglomerates of nanophosphor particles with uniform size distributions are found. At low magnification, long chain-like morphology with polygon shaped nanostructures and sharp boundaries is evidently seen in Fig. 3(b). From TEM observations, the average particle size has been attributed to be in the range of 20–30 nm.

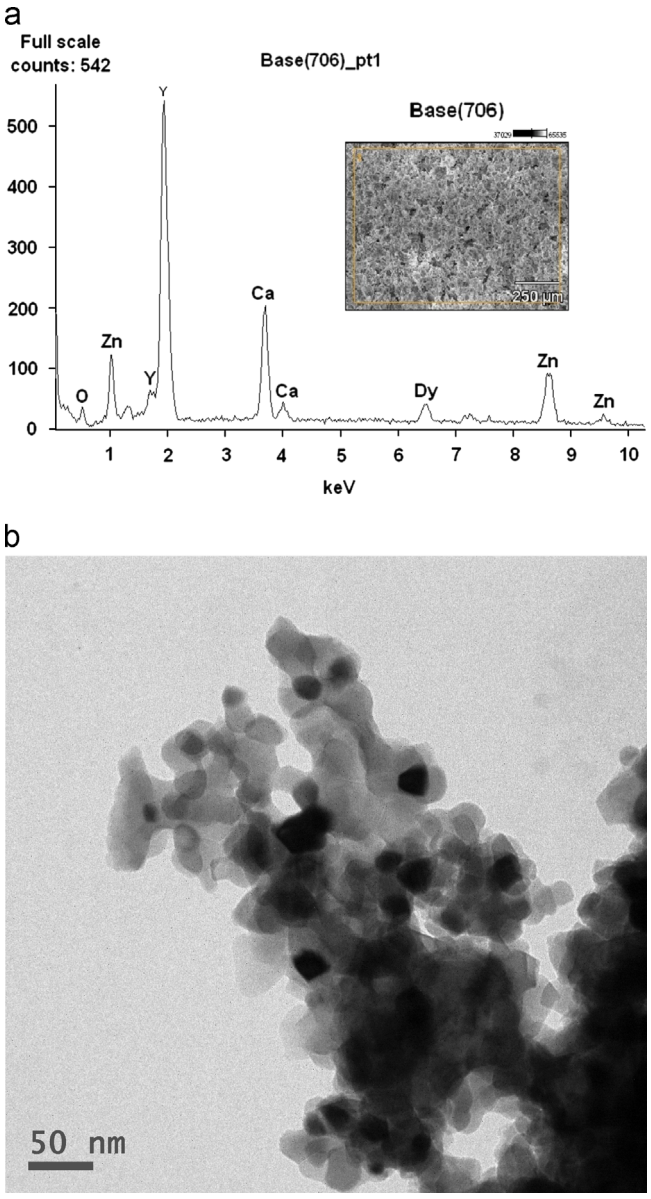

Fig. 3. (a) The energy dispersive x-ray analysis (EDAX) spectra and SEM image (inset) and (b) TEM image of 1.0 mol% Dy_2O_3-doped Y_2CaZnO_5 nanophosphor.

3.2. Photoluminescence properties

Fig. 4 shows the emission spectra with an excitation at 424 nm and also the excitation spectrum obtained by monitoring a yellow emission at 575 nm. The excitation spectra consist of different excitation bands centered at 375 nm ($^6H_{15/2}\rightarrow{}^4F_{7/2}$), 400 nm ($^6H_{15/2}\rightarrow{}^4I_{13/2}$), 424 nm ($^6H_{15/2}\rightarrow{}^4G_{11/2}$), 450 nm ($^6H_{15/2}\rightarrow{}^4I_{15/2}$) and 483 nm ($^6H_{15/2}\rightarrow{}^4F_{9/2}$). The increasing Dy^{3+} ion concentration has no significant effect on the excitation spectra, except a small variation in the intensity. It is interesting to note that the excitation intensity at 424 nm is higher than that of other 4f–4f excitation bands. The excitation bands in the wavelength region of 400–475 nm are found to be stronger in YCZ:Dy^{3+} phosphors than in some of the reported Dy^{3+}-doped phosphors such as $Ca_3Si_2O_7$ [7], $NaGdTiO_4$ [8], $LiSr_4(BO_3)_3$ [9] and $Y_4Al_2O_9$ [10]. As can be seen from the inset of Fig. 4, the YCZ:Dy^{3+} phosphors possess rich excitation bands in the n-UV and blue regions that could be used to efficiently down convert the radiation from the commercial blue emitting InGaN/GaN LED chip which is of significant importance for the development of white-light devices.

Fig. 4 shows the concentration dependent PL emission spectrum of YCZ:Dy^{3+} nanophosphors under 424 nm excitation. The emission spectra consist of two groups of strong peaks in the blue (470–500 nm) and yellow (560–590 nm) regions and a weak band in the red region (660–690 nm), which correspond to the $^4F_{9/2}\rightarrow{}^6H_{15/2}$, $^4F_{9/2}\rightarrow{}^6H_{13/2}$ and $^4F_{9/2}\rightarrow{}^6H_{11/2}$ transitions of Dy^{3+} ions, respectively. The partial energy level diagram shown in Fig. 5 illustrates the excitation and de-excitation processes of Dy^{3+} ions in YCZ nanophosphors. If any level above the $^4F_{9/2}$ level is excited (blue region), a quick non-radiative decay from these levels to the $^4F_{9/2}$ level takes place resulting in a radiative emission from the $^4F_{9/2}$ level. It is worth noting that the variation of

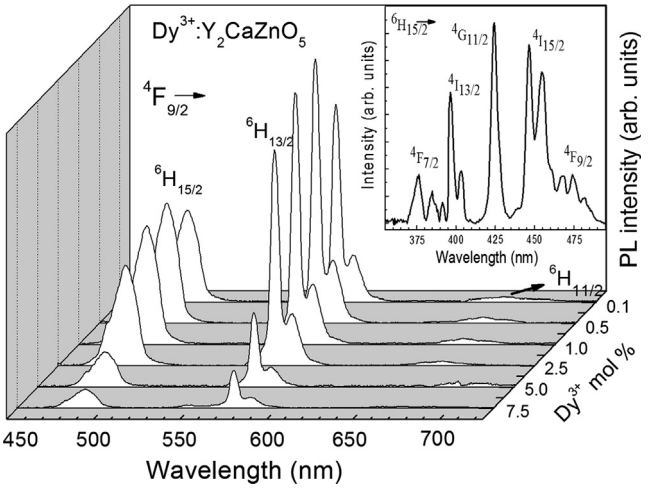

Fig. 4. Concentration dependent emission spectra of Dy_2O_3-doped Y_2CaZnO_5 nanophosphor excited with 424 nm. Inset shows the excitation spectrum of 1.0 mol% Dy_2O_3 doped YCZ by monitoring at 575 nm.

excitation wavelength has no significant effect on the emission profile and hence all the properties were characterized by exciting the samples with 424 nm. The PL spectra are comparable to other Dy^{3+}-doped phosphors such as $Ca_3Si_2O_7$ [7], $NaGdTiO_4$ [8], $LiSr_4(BO_3)_3$ [9] and $Y_4Al_2O_9$ [10]. As can be seen from Fig. 4, the emission intensities of all the three bands increase as the Dy^{3+} ion concentration increases from 0.1 mol% to 1.0 mol% and then quenches at higher (above 1.0 mol%) concentrations and the emission was not observed for the sample with 10 mol% Dy^{3+} ions. The concentration quenching of emission intensity can be attributed to the migration of excited energy to the quenching centers (traps) or to the donors. Based on the Inokuti–Hirayama model analysis of decay times for the $^4F_{9/2}$ level of Dy^{3+} ions, it was concluded that the nature of resonance energy transfer in Dy^{3+}-doped glasses was of the electric dipole–dipole type interaction [13]. The mechanism of concentration quenching of emission intensities can be theoretically modeled based on the integrated intensity (I) of luminescence and the corresponding molar concentration (C) of the activator [14]. According to this relation the interaction type within the activators or between the activator and sensitizer can be estimated from the equation

$$log\left(\frac{I}{C}\right) = -\frac{s}{d}log(C) + log(f) \quad (2)$$

where s is the index of electric multi-pole, which is 6, 8 and 10 for electric dipole–dipole, electric dipole–quadrupole, and electric quadrupole–quadrupole interactions, respectively. If $s=3$, the interaction type is an exchange interaction, d is the dimension of the sample, which can be taken as 3 and f is an independent parameter of doping concentration [14]. Among the electric multi-pole interactions, the slopes of dipole–dipole, dipole–quadrupole and quadrupole-quadrupole are located in [−2,−1], [−8/3,−5/3] and [−10/3,−7/3], respectively. Fig. 6 shows the log(I/C)–log(C) curve of the integrated intensity of $^4F_{9/2}\rightarrow{}^6H_{13/2}$ transition and molar concentration (C) of Dy^{3+} ions in the YCZ systems. From the curve the slope was evaluated from the linear section of the concentration quenching region and is found to be −1.63, which

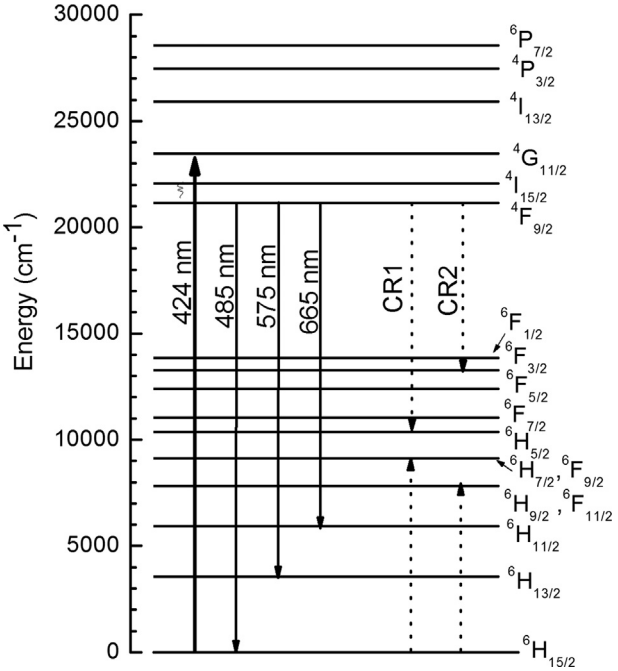

Fig. 5. Partial energy level diagram of Dy^{3+} ions in Y_2CaZnO_5 nanophosphor.

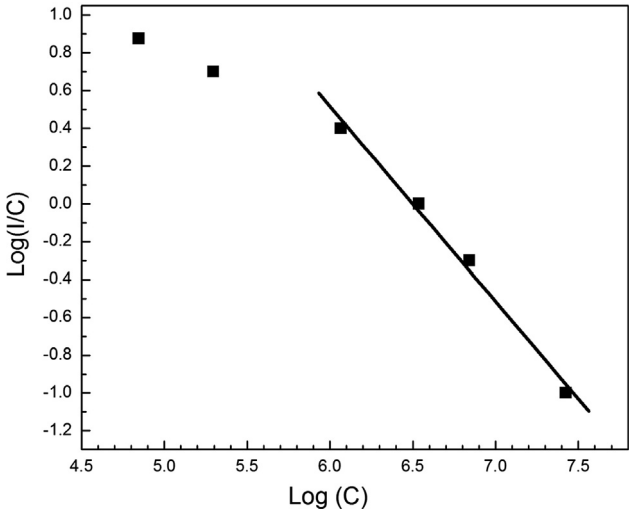

Fig. 6. The relationship between concentration of Dy^{3+} ions (log(C)) and log(I/C) for the $^4F_{9/2}\rightarrow{}^6H_{13/2}$ transition of Dy^{3+} ions in YCZ nanophosphors.

falls in the [−2, −1] block. This indicates that the concentration quenching mechanisms from the $^4F_{9/2}$ level of Dy^{3+} ions in YCZ nanophosphor is of dipole–dipole type, which is consistent with the results obtained for Dy^{3+}: $LiSr_4(BO_3)_3$ [9] and Dy^{3+}: $Sr_3Y_2(BO_3)_4$ [15] phosphors.

3.3. White color properties

Among the visible transitions of Dy^{3+} ions, the blue emission due to $^4F_{9/2}\rightarrow{}^6H_{15/2}$ transition is attributed to the magnetic-dipole in nature, which hardly varies with the crystal-field strength of the host matrix. The yellow emission due to

$^4F_{9/2}\rightarrow{}^6H_{13/2}$ transition is hypersensitive ($\Delta L=2$ and $\Delta J=2$), which is allowed only at low symmetries with no inversion center, moreover, its intensity strongly depends on the host. When Dy^{3+} ion is located at the low-symmetry local site (without an inversion center), the yellow emission is often prominent in the emission spectrum. As the radius of Dy^{3+} (0.103 nm) is almost the same as that of Y^{3+} (0.102 nm), Dy^{3+} ion can easily enter into the Y^{3+} ion site symmetry (without an inversion center). Therefore, for the ions situated at such low symmetry local sites, the $^4F_{9/2}\rightarrow{}^6H_{13/2}$ transition is prominent in their emission spectra. It is feasible to extract white emission by proper adjustment of the two-primary colors emitted from the Dy^{3+} ions at suitable environments.

Table 1 presents the yellow to blue (Y/B) ratios of YCZ:Dy^{3+} nanophosphor with different Dy^{3+} ion concentrations. It is interesting to note that the Y/B ratio is approximately unity (1.08–1.31), and has shown a slight increasing tendency with increase in the Dy^{3+} ion concentration (Table 1), thus indicating the feasibility of generation of white light in YCZ:Dy^{3+} samples. The chromaticity color coordinates of all the investigated samples were calculated and are also shown in Table 1 and the corresponding Commission International de l'Eclairage (CIE) 1931 x–y chromaticity diagram is also presented in Fig. 7. The CIE coordinates of all the investigated samples lie in the near white region, far away from the standard value for white light illumination (0.333, 0.333). On the other hand the CIE coordinates for the other Dy^{3+}-doped systems such as $NaAlSiO_4$ glass-ceramics [5], $LiSr_4(BO_3)_3$ [9], $Sr_3Y_2(BO_3)_4$ [15] and $ZnGa_2O_4$ [16] are found to be well within the white region. It is worth noting that the Dy^{3+}:Y_2O_3 nanophosphor [17] has a CIE coordinate of (0.41, 0.45) which is in the greenish-yellow region. In the present study, the CIE coordinates of the Dy^{3+}:YCZ nanophosphor are found to be shifted close to the white light region.

The light quality of a phosphor for SSL is also evaluated in terms of the correlated color temperature (CCT), which illustrates the temperature of the closest Plankian black-body radiator to the operating point on the chromaticity diagram [18]. Generally, the preferred CCT values range from 3500 to 6500 K, but the range from 3000 to 7800 K is also acceptable. From the CIE chromaticity coordinates, McCamy [19] has proposed the analytical equation to calculate the CCT which is given by

$$\mathrm{CCT} = -449\,n^3 + 3525\,n^2 - 6823.3\,n + 5520.33 \quad (3)$$

where $n=(x-x_e)/(y-y_e)$ is the inverse slope line and ($x_e=0.332$, $y_e=0.186$) is the epicenter. The CCT values obtained for the present Dy^{3+}:YCZ nanophosphor are found in the range of 4386–4491 K, which are comparable to those obtained for YPO_4:Dy^{3+} nanoparticles [6]. These values are slightly more than the warm CCT (i.e., CCT < 4000 K) [18]. The CCT values of the present materials are compared with those of some popular reported systems such as fluorescent tube and day light [20]. The evaluated CCT values of the present materials were found to lie in between those of fluorescent tube (3935 K) and day light (5500 K).

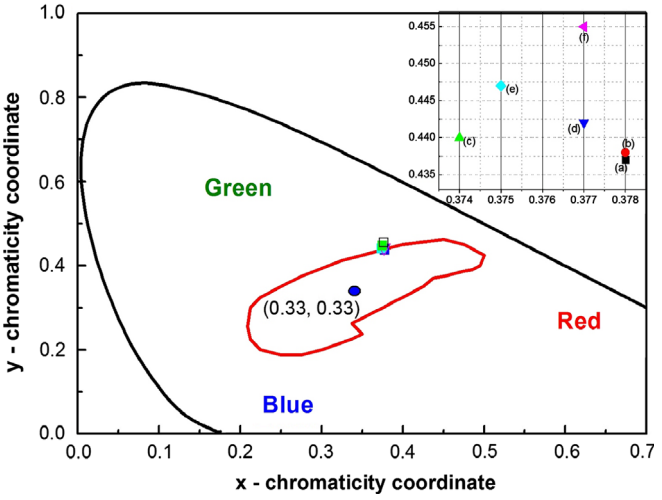

Fig. 7. CIE chromaticity coordinate diagram of Dy_2O_3-doped Y_2CaZnO_5 nanophosphor. Inset shows the expanded view of the CIE diagram, where (a–f) correspond to the studied concentrations (0.1–7.5 mol%).

Table 1
Yellow to blue (Y/B) ratios, lifetimes (μs), CIE chromaticity coordinates and correlated color temperature (CCT, K) obtained for Y_2CaZnO_5 nanophosphors for various concentrations of Dy_2O_3.

Phosphor	Y/B	Lifetimes ± 2%			CIE coordinates		CCT
		τ_1	τ_2	τ_{eff}	x	y	
Dy^{3+}:YCZ (mol%)							
0.1	1.08	532	270	508	0.378	0.437	4392
0.5	1.12	467	214	458	0.378	0.438	4386
1.0	1.08	330	158	479	0.374	0.440	4495
2.5	1.11	190	47	252	0.378	0.442	4410
5.0	1.15	111	7	64	0.375	0.447	4491
7.5	1.31	61	2	–	0.377	0.455	4480
Dy^{3+}:$CaSi_2O_7$ [7]	0.57–0.76	–	–	–	0.330	0.330	5616[a]
Dy^{3+}:$LiSr_4(BO_3)_3$ (1.0 mol%) [9]	0.63	–	–	–	0.261	0.275	12298[a]
Dy^{3+}:$Sr_3Y_2(BO_3)_4$ [15]	0.71–2.92	–	–	–	0.299	0.314	5896
Dy^{3+}:Y_2O_3 (1.0 mol%) [17]	0.42–0.57	–	–	305	0.410	0.450	3800[a]
Dy^{3+}:$ZnGa_2O_4$ [16]	1.0–1.5	–	–	–	0.320	0.330	6114[a]

[a]CCT values calculated from the CIE coordinates reported.

As mentioned above, the abundant excitation peaks of Dy^{3+} ions in the range of 400–475 nm match very well with the commercial blue LED chip, but the chromaticity color coordinates under 424 nm excitation are away from the ideal white light source (0.333, 0.333). Moreover, the Y/B ratio indicates the possibility of extracting white color from the Dy^{3+}:YCZ nanophosphor. All these results indicate that the Dy^{3+}:YCZ nanophosphor is a promising candidate for the generation of white light when coupled with a blue LED chip; however, the chromaticity color coordinates need to be improved by modification of the host composition to enhance the red emission part.

3.4. Lifetime measurements

Fig. 8 shows the luminescence decay curves of the intense luminescent $^4F_{9/2}\rightarrow{}^6H_{13/2}$ transition of Dy^{3+} ions in YCZ nanophosphors for various concentrations of Dy^{3+} ions. For lower concentrations, the fluorescence decay curves are found to be nearly single exponential in nature and as the concentration increases they tend to deviate from this behavior. The non-exponential behavior of decay from the $^4F_{9/2}$ level of Dy^{3+} ions is also found in other reported Dy^{3+}-doped phosphors [8]. The decay curves have been well fitted to the following bi-exponential function:

$$I(t) = A_1 exp(-t/\tau_1) + A_2 exp(-t/\tau_2) \quad (4)$$

The non-exponentiality in the decay curves of Dy^{3+}-doped materials usually arises from ion–ion interactions due to energy transfer from the activator to the impurities and cross-relaxation processes. The lifetime (τ_{eff}) for both the near single exponential and non-exponential decay curves has been evaluated using the following expression and the results are listed in Table 1.

$$\tau_{eff} = \frac{\int tI(t)dt}{\int I(t)dt} \quad (5)$$

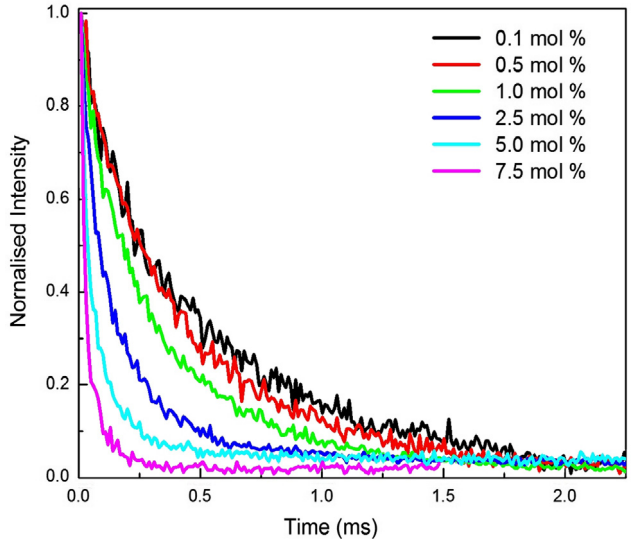

Fig. 8. Concentration dependent decay profiles of the $^4F_{9/2}$ level of Dy^{3+} ions in Y_2CaZnO_5 nanophosphor obtained with an excitation of 424 nm.

As can be seen from Table 1, the variation in the decay components is very quick at higher concentrations which indicates the enhancement in the energy transfer process. At higher concentration of Dy^{3+} ions (7.5 mol%), the decay was very short and hence the estimation of lifetime was not straightforward due to dominant measurement error.

Since the interaction between Dy^{3+}–Dy^{3+} ions is negligible at lower concentration, the fluorescence decay is nearly single exponential. However, when the concentration is large enough, the interaction between Dy^{3+}–Dy^{3+} ions becomes predominant and energy transfer processes from a donor (excited Dy^{3+} ion) to an acceptor (ground Dy^{3+} ion) come into picture that lead to a prolonged the non-exponential decay. The enhancement of non-exponential nature of the decay curves, with increase in Dy^{3+} ion concentration can be further explained due to resonant or nearly resonant energy transfer from the Dy^{3+} ion in an excited $^4F_{9/2}$ state to a nearby Dy^{3+} ion in the ground $^6H_{15/2}$ state. This transfer leaves the first ion in the intermediate level of $^6H_{9/2}$ (at ~1275 nm) and the second one in $^6F_{1/2}$ (at ~720 nm) level which occur in resonance with $^4F_{9/2}\rightarrow{}^6H_{9/2}$ (at ~730 nm) transitions. Later both the ions quickly decay non-radiatively to the ground state. Resonant or nearly resonant cross-relaxation channels which can account for this energy transfer process are

$$^4F_{9/2} + {}^6H_{15/2} \rightarrow {}^6H_{5/2} + {}^6H_{7/2}$$

$$^4F_{9/2} + {}^6H_{15/2} \rightarrow ({}^6F_{3/2},\ {}^6F_{1/2}) + ({}^6H_{9/2},\ {}^6F_{11/2})$$

These cross-relaxation channels are shown in the partial energy level diagram (Fig. 5, dotted arrows) as CR1 and CR2, correspondingly.

4. Conclusions

To conclude, new and novel two primary colors (blue and yellow) emitting nanophosphor, Y_2CaZnO_5 (YCZ) doped with Dy^{3+} ions, was prepared by the modified citrate gel combustion method. Intense and broad excitation peaks of Dy^{3+}:YCZ nanophosphors were observed in the 420–450 nm region which match very well with the emission wavelength of the commercially available low cost blue LED chips. The analysis of concentration dependent luminescent properties of Dy^{3+}:YCZ nanophosphor indicates that 1.0 mol% of Dy^{3+} ions is the ideal activator concentration. The study of white color properties, such as CIE chromaticity coordinates, Y/B ratios and CCT values, reveals that the Dy^{3+}:YCZ nanophosphor is a suitable candidate for the generation of white-light from the blue LED chip.

Acknowledgments

One of the authors (C.K.J) is grateful to the Governments of India and Spain for the award of a project within the Indo-Spanish Joint Programme of Cooperation in Science and Technology (DST-INT-Spain-P-38–11 and PRI-PIBIN-2011–1153) and UGC (F.40–435/2011 (SR)); Govt. of India, for the sanction of major research projects.

References

[1] Lei Chen, Chun-Che Lin, Chiao-Wen Yeh, Ru-Shi Liu, Light converting inorganic phosphors for white light-emitting diodes, Materials 3 (2010) 2172–2195.

[2] D. Haranath, Harish Chander, Pooja Sharma, Sukhvir Singh, Enhanced luminescence of $Y_3Al_5O_{12}:Ce^{3+}$ nanophosphor for white light-emitting diodes, Applied Physics Letters 89 (173118) (2006) 1–3.

[3] Koen Van den Eeckhout, Philippe F. Smet, Dirk Poelman, Persistent luminescence in Eu^{2+}-doped compounds: a review, Materials 3 (2010) 2536–2566.

[4] T.W. Kuo, W.R. Liu, T.M. Chen, High color rendering white light-emitting-diode illuminator using the red-emitting Eu^{2+}-activated CaZnOS phosphors excited by blue LED, Optics Express 18 (2010) 8187–8192.

[5] Ruchika Bagga, Venu Gopal Achanta, Ashutosh Goel, Jose M.F. Ferreira, Narinder Pal Singh, Davinder Paul Singh, Mauro Falconierig, Gopi Sharma, Dy^{3+}-doped nano-glass ceramics comprising $NaAlSiO_4$ and $NaY_9Si_6O_{26}$ nanocrystals for white light generation, Materials Science and Engineering: B 178 (2013) 218–224.

[6] A.K. Parchur, A.I. Prasad, S.B. Rai, R.S. Ningthoujam, Improvement of blue, white and NIR emissions in $YPO_4:Dy^{3+}$ nanoparticles on co-doping of Li^+ ions, Dalton Transactions 41 (2012) 13810–13814.

[7] Xinghua Zhang, Zunming Lu, Fanbin Meng, Long Hu, Xuewen Xu, Jing Lin, Chengchun Tang, Luminescence properties of $Ca_3Si_2O_7:Dy^{3+}$ phosphor for white light-emitting diodes, Materials Letters 79 (2012) 292–295.

[8] Hua Zhong, Xiangping Li, Rensheng Shen, Jinsu Zhang, Jiashi Sun, Haiyang Zhong, Lihong Cheng, Yue Tian, Baojiu Chen, Spectral and thermal properties of Dy^{3+}-doped $NaGdTiO_4$ phosphors, Journal of Alloys and Compounds 517 (2012) 170–175.

[9] Zhi-Wei Zhang, Xin-Yuan Sun, Lu Liu, You-shun Peng, Xi-hai Shen, Wei-Guo Zhang, Dong-Jun Wang, Synthesis and luminescence properties of novel $LiSr_4(BO_3)_3:Dy^{3+}$ phosphors, Ceramics International 39 (2013) 1723–1728.

[10] Z. Boruc, B. Fetlinski, M. Malinowski, S. Turczynski, D. Pawlak, Optical transitions intensities of $Dy^{3+}:Y_4Al_2O_9$ crystals, Optical Materials 34 (2012) 2002–2007.

[11] S. Ye, F. Xiao, Y.X. Pan, Y.Y. Ma, Q.Y. Zhang, Phosphors in phosphor-converted white light-emitting diodes: recent advances in materials, techniques and properties, Materials Science and Engineering: R 71 (2010) 1.

[12] A. Tanner, Ka Leung Wong, Synthesis and spectroscopy of lanthanide ion-doped Y_2O_3, Journal of Physical Chemistry B 108 (2003) 136.

[13] C.K. Jayasankar, V. Venkatramu, S. Surendra Babu, P. Babu, Luminescence properties of Dy^{3+} ions in a variety of borate and fluoroborate glasses containing lithium, zinc, and lead, Journal of Alloys and Compounds 374 (2004) 22.

[14] Xin-yuan Sun, Shi-ming Huang, Xiao-san Gong, Qing-chun Gao, Zi-piao Ye, Chun-yan Cao, Spectroscopic properties and simulation of white-light in Dy^{3+}-doped silicate glass, Journal of Non-Crystalline Solids 356 (2010) 98–101 and references there in.

[15] Panlai Li, Zhiping Yang, Zhijun Wang, Qinglin Guo, White-light-emitting diodes of UV-based $Sr_3Y_2(BO_3)_4:Dy^{3+}$ and luminescent properties, Materials Letters 62 (2008) 1455–1457.

[16] K. Mini Krishna, G. Anoop, M.K. Jayaraj, Host sensitized white luminescence from $ZnGa_2O_4:Dy^{3+}$ phosphor, Journal of Electrochemical Society 154 (2007) J310–J313.

[17] M. Jayasimhadri, B.V. Ratnam, Kiwan Jang, Ho Sueb Lee, Baojiu Chen, Soung-Soo Yi, Jung-Hyun Jeong, L. Rama Moorthy, Greenish-yellow emission from Dy^{3+}-doped Y_2O_3 nanophosphors, Journal of American Ceramic Society 93 (2010) 494–499.

[18] T. Erdem, S. Nizamogul, X.W. Sun, H.V. Demir, A photometric investigation of ultra-efficient LEDs with high color rendering index and high luminous efficacy employing nanocrystal quantum dot luminophores, Optics Express 18 (2010) 340–347.

[19] C.S. McCamy, Correlated color temperature as an explicit function of chromaticity coordinates, Color Research and Application 17 (1992) 142–144.

[20] Ingo Speier, Marc Salsbury, Color temperature tunable white light LED system, Proceedings of SPIE 6337 (2006) 63371F-1–63371F-12.